DYNAMIC BEHAVIOR IMPROVEMENT OF INDUCTION HEATING CONVERTERS USING FUZZY LOGIC CONTROLLER

ANAND KUMAR[1], RAHUL RAMAN[1], PRADIP KUMAR SADHU[1]

In induction heating (IH) system, it has been observed that, due to load variation, the effective voltage across the load changes. Owing to this, resonance condition is affected and also the desired output power across the load starts to vary. It is essential to maintain resonance condition and constant output power to IH load in order to enhance its heating quality. Regarding this requirement, this paper approaches a design of fuzzy logic controller (FLC) using pulse density modulation (PDM) technique for full bridge series resonant inverter (FB-SRI) to maintain constant output power irrespective of load variation for IH applications. The proposed technique has been validated in MATLAB/Simulink environment under different load parameters. The results are obtained through simulation and this shows the uniqueness of the FLC using PDM to maintain the constant output power across the load.

1. INTRODUCTION

In the past few years, it has been observed that for industrial as well as domestic applications, IH system is the most popular choice as compared to other classical heating methods such as convection, conduction, and radiation. IH techniques offer many advantages like high efficiency, more reliability, both environment and user-friendly [1, 2]. In this type of system, power should be accurately and smoothly controlled in order to get uniform temperature across the load of IH [3]. The power across the load of IH is controlled by means of resonant converter.

For designing of an IH system, resonant converter plays a vital role to generate a high-frequency (HF) current [4, 5]. There are numerous topologies relating to this converter that have been developed such as a class D resonant inverter, series resonant inverter, single switch resonant inverter (Flyback inverter), modified single switch resonant inverter, half and full bridge topology [6–9]. Among all these topologies, generally FB-SRI is being employed due to its capability of sustaining high voltage or high current and its high switching frequency (Fig. 1) [10, 11]. All the resonant inverters operate at the resonant frequency (switching frequency) or nearly around (more or less than) the resonant frequency in order to get zero voltage switching (ZVS) or zero current switching (ZCS) [8, 11]. Along with these resonant converter topologies, also there are lots of power control techniques that have been created [13, 14]. Each has its own advantages and disadvantages. However, no single method is able to improve the dynamic behavior of the resonant converter topologies along with the consideration of variation of the load in IH system or input voltage for the inverter. As an example, in rural areas of India or other developing countries, power quality/supply to the consumer is not so good. Because of this, input supply for the resonant converter always varies, as a result of this, uniform heating across the load does not occur [15]. The variation in equivalent impedance of load and coil is the other reason which leads us to study the dynamic behavior of IH system. Due to this, effective voltage which is applied to work coil automatically decreases. It has been found that the cause of decrement in effective voltage is a change in steady state temperature, change in resonant frequency or change in alignment between work coil and load [16, 17]. To maintain the load voltage constant without disturbance in resonant frequency/operation of the resonant inverter, closed loop designing will be the better choice. For the designing of closed loop system to maintain constant load voltage regardless of variation in input voltage or change in load parameters, fuzzy logic plays a vital role [18]. So many methods for designing of closed-loop system like proportional integral (PI), proportional integral derivative (PID) etc have been developed but these methods don't seem to be able to maintain constant output voltage/current for non-linear load. Also its accuracy is less and takes more response time.

In this work, a FLC for FB-SRI has been developed which improves the dynamic behavior of the converter. This proposed system using artificial intelligence (*i.e.* fuzzy logic), has been verified using MATLAB/Simulink environment under different loading conditions. Also, this proposed system is able to maintain constant output average power (P_{ave}) at the variations of load within some acceptable range. For analyzing the dynamic behavior of this converter, transient response equation for voltage, current and power have been derived.

The rest part of this work is as follows: in Section 2, the proposed FB-SRI using FLC and its transient analysis have been described. Design of FLC for IH applications associated with PDM technique has been analyzed in Section 3. Various simulated results and its analysis have been presented in Section 4. Finally conclusion for this work is drawn in Section 5.
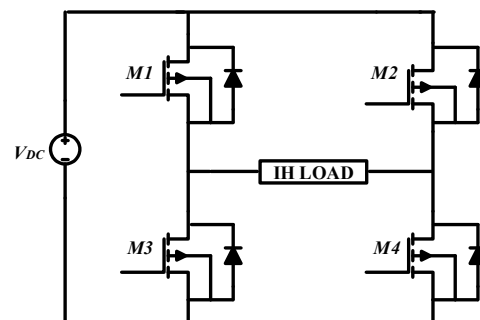

Fig. 1 – FB-SRI for IH applications.

[1] Indian Institute of Technology (Indian school of Mines), Dhanbad, Jharkhand 826004, India; E-mail: anand.2016dr0084@ee.ism.ac.in
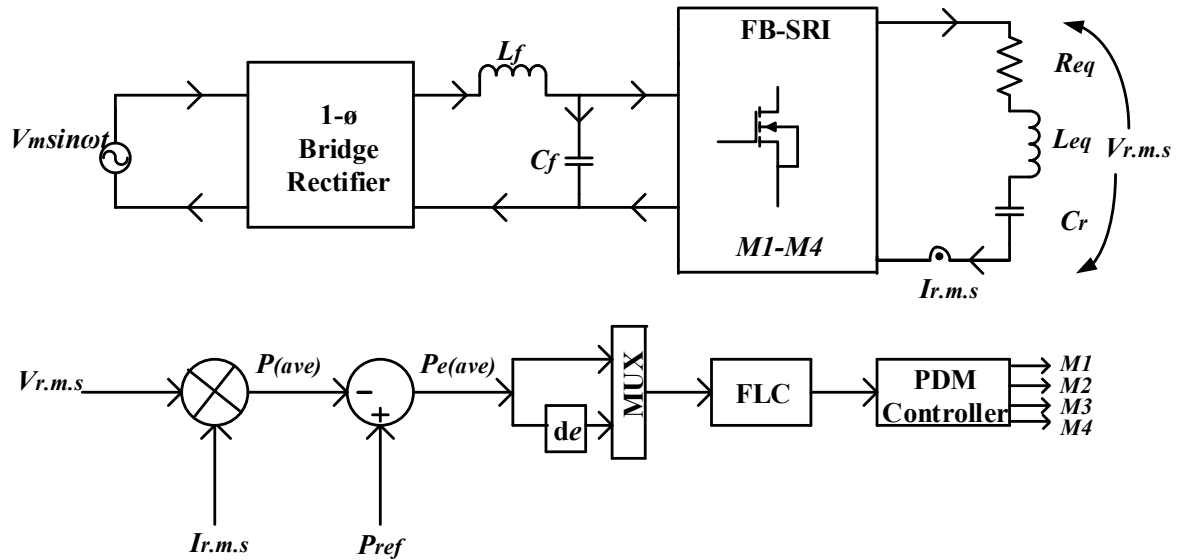
Fig. 2 – Block diagram of proposed fuzzy logic based FB-SRI for IH applications.

2. PROPOSED FUZZY LOGIC BASED FB-SRI

The block diagram of proposed fuzzy logic based FB-SRI is shown in the Fig. 2. This is basically a two-stage converter for converting grid frequency ac (50 Hz) to high-frequency ac (HF ac) to satisfy the desired criteria for IH applications. From the block diagram, it can be seen that, in the first stage, 1-ø ac supply is converted to dc supply. Then dc link capacitor (C_f) and inductor (L_f) is used to remove the ripple content in the output of bridge rectifier. IH needs a HF ac, so for this in the second stage, the pure dc supply is again converted to HF ac with the help of FB-SRI. This HF ac flows through the load coil of IH which is shown in Fig. 3, so that pot or work piece gets heated.

For analyzing the electrical behavior of the IH system, IH coil is modeled as the series connection of equivalent resistance (R_{eq}) and equivalent inductance (L_{eq}) which is shown in the Fig. 3. Also, resonant capacitor (C_r) is used to create resonance condition which is either connected in series or in parallel having the combination of R_{eq} and L_{eq}. M1 to M4 are the MOSFET switches which is used in designing for FB-SRI (Fig. 1). These switches *i.e.* M1, M4 and M2, M3 are alternately turn ON and OFF according to the pulse applied through PDM technique using FLC scheme. By using FLC, the variation in dc supply for resonant inverter or change in load, output power remains constant as reference power (P_{ref}) set by the user.
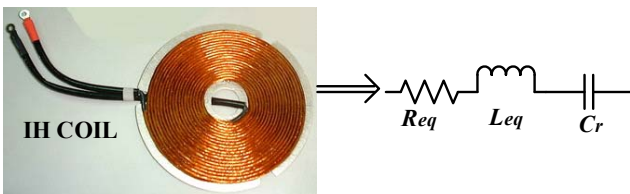

Fig. 3 – Electrical modeling of IH coil.

2.1. TRANSIENT ANALYSIS OF INDUCTION HEATING SYSTEM

It is already aforementioned that, HF ac is applied to the IH coil. So to analyze the electrical behavior of the IH system, detailed modeling is shown in Fig. 4. In this circuit (Fig. 4a), R_c is the coil resistance which is very small as

compared to load resistance (R_L). L_c, L_s, and M are the coil, self, and mutual inductance. $R_{eq} = \{R_C + R_L(n1/n2)^2\}$ and $L_{eq} = \{L_C + L_S (n1/n2)^2 \}$ are the equivalent resistance and capacitance which is obtained by referring secondary value to primary side shown in Fig. 4b. I is the total load current (secondary referred to primary) flowing through the circuit which might be the eddy current (responsible for generating heat in the pot).
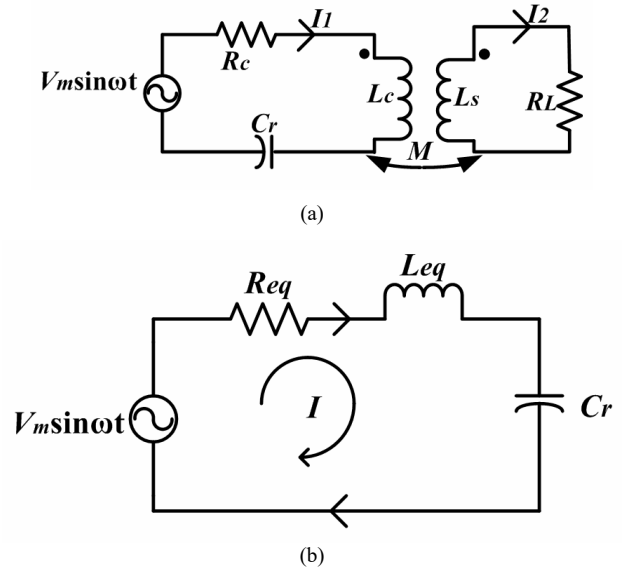

(a)

(b)

Fig. 4 – Equivalent electrical modeling of IH load.

$$V_m \sin \omega t = R_{eq} \times I + L_{eq} \frac{\mathrm{d}I}{\mathrm{d}t} + \frac{1}{C_r} \int I \mathrm{d}t \ , \qquad (1)$$

$$V_{R_{eq}} = R_{eq} \times I \ . \qquad (2)$$

Taking Laplace transform both sides for equations (1) and (2)

$$V_m \frac{\omega}{(s^2 + \omega^2)} = R_{eq} I(s) + L_{eq} s I(s) + \frac{I(s)}{sC_r} \ , \qquad (3)$$

$$V_{R_{eq}} (s) = R_{eq} I(s) , \qquad (4)$$

$$I(s) = \frac{V_{R_{eq}} (s)}{R_{eq}} \ . \qquad (5)$$

On putting the value of equation (5) in equation (3)

$$V_m \frac{\omega}{(s^2+\omega^2)} = V_{Req}(s) + \frac{sL_{eq}V_{Req}(s)}{R_{eq}} + \frac{V_{Req}(s)}{sC_rR_{eq}} \quad (6)$$

$$V_{Req}(s) = \frac{V_m\left\{\dfrac{\omega}{(s^2+\omega^2)}\right\}}{\left(\dfrac{1}{sC_rR_{eq}} + \dfrac{sL_{eq}}{R_{eq}} + 1\right)} \quad . \quad (7)$$

Roots of denominators can be calculated as

$$s_1, s_2 = -\frac{R_{eq}}{2L_{eq}} \pm \sqrt{\left(\frac{R_{eq}}{2L_{eq}}\right)^2 - \frac{1}{L_{eq}C_{eq}}} \quad . \quad (8)$$

On putting the values of denominator roots in equation (7)

and by taking $P = -\dfrac{R_{eq}}{2L_{eq}}, j\omega^* = \sqrt{\left(\dfrac{R_{eq}}{2L_{eq}}\right)^2 - \dfrac{1}{L_{eq}C_{eq}}}$

where ω^* is the angular switching frequency

$$V_{Req}(s) = \frac{s\left(\dfrac{R_{eq}}{L_{eq}}\right)}{\{(s+p)^2+(\omega^*)^2\}} \times V_m \frac{\omega}{(s^2+\omega^2)} \quad (9)$$

$$= V_m \frac{R_{eq}}{L_{eq}} \frac{s\omega}{\{(s+p)^2+\{\omega^*\}^2\}(s^2+\omega^2)}.$$

Normally, it has been seen that IH system need underdamped response to create ZVS condition in order to reduce switching losses across the power electronics switches. So for this, switching frequency (f_s) should be kept at somewhat higher than resonant frequency (f_r). Because of this, all these equations are analyzed on the assumption of underdamped response *i.e.* $\left(\dfrac{R_{eq}}{2L_{eq}}\right)^2 < \dfrac{1}{L_{eq}C_{eq}}$. Also, heat generation in the IH system is directly related to power transferred to the load by the resonant converter. So for maximum generation of heat, maximum power should be transferred and it can happen when switching frequency (f_s) will be equal to the resonant frequency (f_r). Owing to this, for further analyzing of transient equations, $\omega^* = \omega$ has been taken.

Now again

$$V_{Req}(s) = V_m \frac{R_{eq}}{L_{eq}} \frac{s\omega}{\{(s+p)^2+(\omega)^2\}(s^2+\omega^2)} \quad (10)$$

On solving equation (10) using partial fraction and some Laplace inverse manipulations,

$$V_{Req}(t) = V_m \frac{R_{eq}}{L_{eq}} \frac{1}{(p^2+4\omega^2)}$$

$$\times \left\{(1-\omega e^{-pt})\cos\omega t + \frac{2\omega^2-\{p^2+2\omega^2\}e^{-pt}}{p}\sin\omega t\right\}. \quad (11)$$

From the equation (11), it can be concluded that with the variations in input voltage (V_m) or load *i.e.* R_{eq} or L_{eq}, the magnitude of the output voltage across the IH load will change. So to maintain constant output or effective voltage across the IH load, the FLC has been proposed in this work which is discussed in next section.

3. FLC BASED IH SYSTEM USING PDM TECHNIQUE

In order to maintain constant output power irrespective of the change in input supply voltage or load within some acceptable range, the FLC has been proposed in this work. The advantages of FLC are that it can be used for both linear as well as a nonlinear system; also it does not require mathematical modeling as comparison to another controller.

From the block diagram, as shown in Fig. 2, the output R.M.S voltage ($V_{r.m.s}$) and current ($I_{r.m.s}$) is sensed to generate average output power (P_{ave}) and it is compared with desired reference average power (P_{ref}) in order to generate the error between average power *i.e.* error in average power ($P_{e(ave)}$) and reference average power (P_{ref}).

This error is divided into two parts i.e. error and change in error which act as an input for FLC. Now, the output of FLC is used to control the duty cycle of PDM (α_{PDM}). The detailed block diagram of FLC is shown in Fig. 5 which is divided into three steps: fuzzifications, decision making, and defuzzification. In the first step *i.e.* fuzzification, the numerical value (or crisp value) is converted into a linguistic variable. The controlling inputs for fuzzification process are error ($P_{k_{e(ave)}}$) and change in error ($cP_{k_{e(ave)}}$) which can be defined as follows:-

$$P_{k_{e(ave)}} = P_{ref(ave)} - P_{ave} , \quad (12)$$

$$cP_{k_{e(ave)}} = P_{k_{e(ave)}} - P_{(k-1)e(ave)} . \quad (13)$$
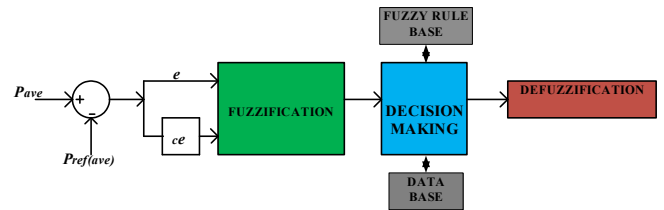

Fig. 5 – Detailed block diagram FLC structure.

The output of the FLC is defined as:-

$$P_{dk} = P_{d(k-1)} + n\delta P_{dk} , \quad (14)$$

where

δP_{dk} is the inferred change of the fuzzy output,

P_{dk} is the power at k^{th} sampling,

n is the gain of FLC which is adjustable to control the gain of the controller.

Now in the second step i.e. decision making which is associated with fuzzy rule base and database, define the relationship between fuzzy input and output sets. A fuzzy rule is defined by knowing the system behavior and simply If-Then condition is used to make fuzzy rules. There are total of 25 fuzzy rules have been created for this proposed work which is shown in Table. I. There are five fuzzy levels have been chosen in order to control error and change in error: large positive (LP), small positive (SP), zero (Z), small negative (SN), and large negative (LN). Also, two extra output variable is added: medium negative (MN) and medium positive (MP). The membership function (μ_f) is defined in the normalized range of [–1, 1] which is shown Fig. 6.
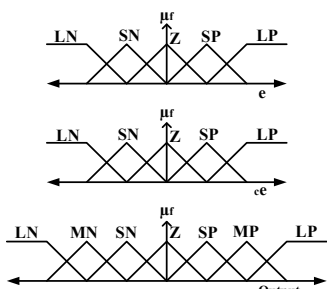
Fig. 6 – Membership function (μ_f).

Fig. 7 – Block diagram for generation of gate pulses through PDM technique.

Following linguistic assumptions has been taken to design fuzzy rules:

- If the $P_{e(ave)}$ is large, then change in α_{PDM} should also be large to bring the output P_{ave} to the P_{ref}.

- If the $P_{e(ave)}$ is nearly zero, then a little bit change in α_{PDM} will be needed.

- If the $P_{e(ave)}$ is nearly zero and change in error ($cP_{k_{e(ave)}}$) is large, then α_{PDM} should be maintained constant.

- If the $P_{(ave)}$ reaches P_{ref} with some fluctuation, then α_{PDM} should be maintained small to avoid moving P_{ave} from its reference power *i.e* P_{ref}.

By using the above listed linguistic assumption, about 25 (5×5) fuzzy rules have been developed which are shown in Table 1. Now the last stage is defined as defuzzification which fuzzified value is converted into crisp value (numerical value) in normalized range. For defuzzification, centroid or centre of area technique is used in this work which is defined as $P = \dfrac{\sum \mu_x P_x}{\sum \mu_x}$, where P represents the crisp value and μ is the membership function.

By using above defined steps, an FLC has been designed which is able to maintain constant output power of resonant inverter.

Table 1
Fuzzy rule

e/ce	LN	SN	Z	SP	LP
LN	MN	SP	LN	MP	LN
SN	MP	LP	MP	LN	SN
Z	MP	SP	Z	LN	SN
SP	LN	LP	MN	LP	Z
LP	MN	MP	SN	LN	LZ

3.1. PDM TECHNIQUE

It is aforesaid in the above section that output of FLC goes to PDM controller which is responsible for controlling duty cycle (α_{PDM}). In this subsection, some brief overview on PDM controller is discussed. In this type of control, switching frequency (f_s) should be kept constant and this switching frequency must be greater than resonant frequency (f_r) to create ZVS condition. Figure 7 shows the generation of gate signals through PDM technique. From this figure it can be seen that HF and low-frequency signal are logically compared to generate the gate signal for MOSFETs M1 to M4.
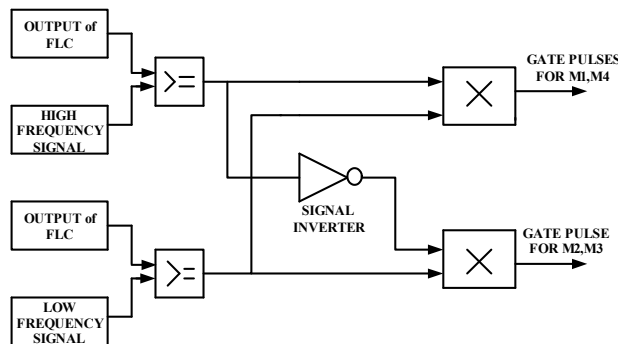
The duty cycle of PDM controller is defined as

$$\alpha_{PDM} = \frac{t_{ON}}{t_{PDM}} \quad , \tag{15}$$

where t_{ON} and t_{OFF} is the turn ON turn OFF time period of the PDM pulses respectively.

The output average power can be controlled as

$$P_{ave} = \frac{t_{ON}}{t_{PDM}} P_{ref} \quad , \tag{16}$$

$$P_{ave} = \frac{Q}{t} = \frac{mC\Delta T}{t} \quad , \tag{17}$$

$$Q = P_{ave} \times t \quad , \tag{18}$$

$$Q = \alpha_{PDM} \times P_{ref} \times t \quad , \tag{19}$$

where Q is heat energy generated across load in joules (J),
m is the mass/volume of object to be heated in grams (g) or litre (l),
C is the specific heat of object to be heated in (J/g),
t is the time in second (s),
ΔT is the change in temperature.

Equations (17) to (19) represent heat generated across the load in terms of power which can be regulated by duty cycle of PDM (α_{PDM}).

4. SIMULATION MODEL, RESULTS AND IT'S DISCUSSION

To validate the aforementioned proposed technique, simulation has been done using MATLAB/Simulink environment and various waveforms of load voltage (V_{out}), load current (I_{out}), and average output power (P_{ave}) have been taken to analyze the proposed system behavior. It is already discussed in above section that, whenever pot is kept over the coil or work piece is kept inside the coil, the effective output voltage decreased due to change in equivalent parameters. Owing to this output average power (P_{ave}) changes. In this work, FLC has been designed and simulated to maintain constant output, average power (P_{ave}) at different values of the load is shown in Table 2. This FLC aided PDM controller maintains minimum switching losses for the wide load range variation. Along with it, this scheme is also able to support the input voltage variation within acceptable limit. For analyzing the system behavior, a simulation study has been done in two ways: with FLC or without FLC at different values of R_{eq} and L_{eq}. If the $P_{e(ave)}$ is large, then change in α_{PDM} should also be large to bring the output P_{ave} to the P_{ref}.

Table 2

Output average power (P_{ave}) at different variation of load parameters at V_{in} = 100 V, P_{ref}= 100 W, f_s=25 kHz

$R_{eq}(\Omega)$	L_{eq}(mH)	P_{ave}(W) (without FLC)	P_{ave}(W) (with FLC)
15	0.3	166.1	99.43
20	0.4	140.9	99.44
25	0.5	121.7	99.46
30	0.6	108	99.44

Table 2 illustrates the output average power with or without FLC at different load parameters keeping V_{in} = 100 V, P_{ref}=100 W, and f_s= 25 kHz (*i.e.* high-frequency signal or resonant frequency). From the Table 2, it can be observed that, with the variation in load, P_{ave} is not changing when FLC is used and it is very close to reference power (P_{ref}) as compared to P_{ave} without FLC. Figures 8 and 9 depict the simulation results of V_{out}, I_{out} and P_{ave} at a load of R_{eq} = 20 Ω, L_{eq} = 0.4 mH to R_{eq} = 30 Ω, L_{eq}= 0.6 mH. From the Figs 8 and 9, it can be seen that there is no much difference in waveforms of voltage, current, and power. However from the close observation, the simulated current waveform changes in accordance with the load but the simulated voltage waveform remain same along with steady state average power because of FLC controller. So, it can be concluded that the output average power (P_{ave}) remains constant using FLC. Figure 10 shows the pulse generated (which is given to the MOSFETs of the FB-SRI) by FLC aided PDM controller.
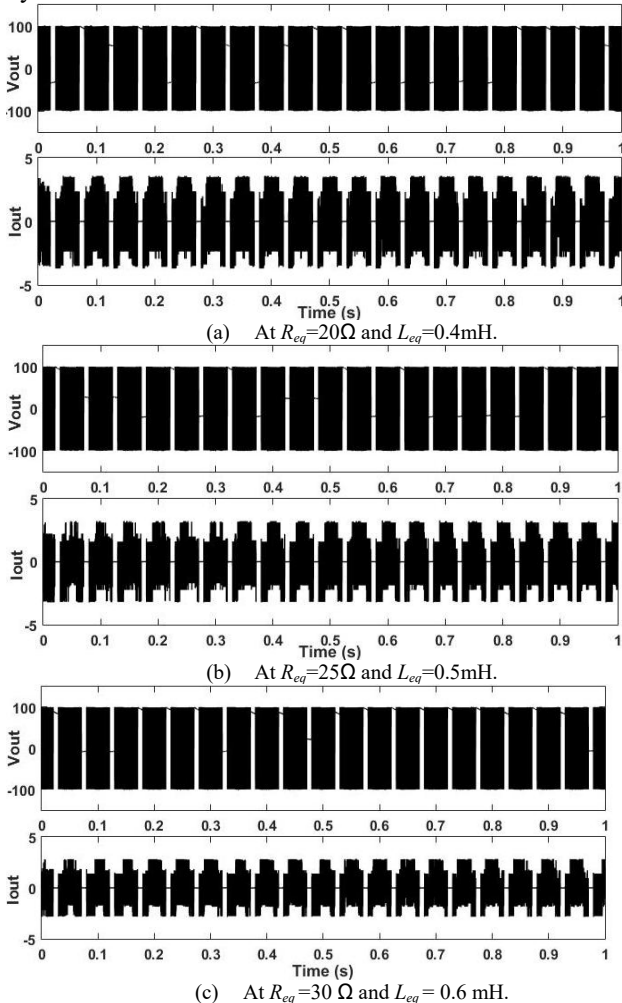
(a)　　At R_{eq}=20Ω and L_{eq}=0.4mH.

(b)　　At R_{eq}=25Ω and L_{eq}=0.5mH.

(c)　　At R_{eq}=30 Ω and L_{eq} = 0.6 mH.

Fig. 8 – Simulated results of load voltage (V_{out}) and load current (I_{out}) at different load parameters using FLC.

(a)　　At R_{eq}=20 Ω and L_{eq}=0.4 mH.

(b)　　At R_{eq}=25 Ω and L_{eq}=0.5 mH.
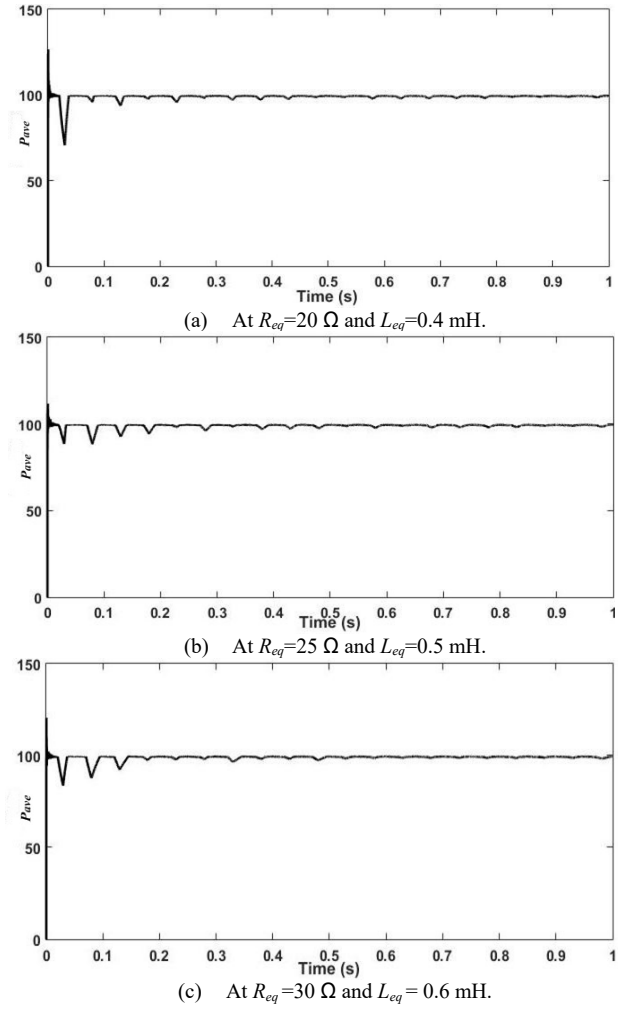
(c)　　At R_{eq}=30 Ω and L_{eq} = 0.6 mH.

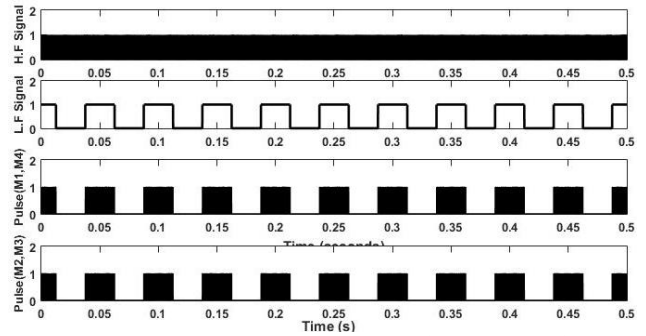Fig. 9 – Simulated results of output average power (P_{ave}) at different load parameters using FLC.

Fig. 10 – Simulated result of pulse generation though PDM technique using FLC.

5. CONCLUSION

In this work FLC aided PDM based FB-SRI for IH applications has been proposed to maintain constant output power. Some mathematical modeling has been done to show the dynamic nature of IH system. The performance of the proposed technique is studied under different variation of load conditions. To validate this proposed technique, simulation has been done using MATLAB/Simulink environment which shows that, FLC is able to maintain constant output power. The proposed technique can be used for both domestic as well as industrial IH applications and it also increases the power efficiency along with the control accuracy.

REFERENCES

1. O. Lucía, P. Maussion, E. Dede, J.M. Burdío, *Induction heating technology and its applications: Past Developments, current Technology, and future challenges*, IEEE Trans. Ind. Electron., **61**, *5*, pp. 2509–2520 (2014).

2. J. Acero, J.M. Burdio, L.A. Barragán, *et al, The domestic induction heating appliance: An overview of recent research*, Conf. Proc. - IEEE Appl. Power Electron. Conf. Expo. - APEC, pp. 651–657 (2008).

3. Z. Ye, P.K. Jain, P.C. Sen, *A full-bridge resonant inverter with modified phase-shift modulation for high-frequency AC power distribution systems*, IEEE Trans. Ind. Electron, **54**, *5*, pp. 2831–2845 (2007).

4. H. Sarnago, Ó. Lucía, J. M. Burdío, *Interleaved Resonant Boost Inverter Featuring SiC Module for High-Performance Induction Heating*, IEEE Trans. on Power Electron., **32**, *2*, pp. 1018–1029 (2017).

5. T. Mishima, S. Sakamoto, C. Ide, *ZVS Phase-Shift PWM-Controlled Single-Stage Boost Full-Bridge AC–AC Converter for High-Frequency Induction Heating Applications*, IEEE Trans. on Ind. Electron., **64**, *3*, pp. 2054–2061 (2017).

6. H. Sarnago,O. Lucía, A. Mediano, J.M. Burdío, *Class-D/DE dual-mode-operation resonant converter for improved-efficiency domestic induction heating system,* IEEE Trans. Power Electron., **28**, *3*, pp. 1274–1285 (2013).

7. A. Shenkman, B. Axelrod, Y. Berkovich, *Improved modification of the single-switch AC-AC converter for induction heating applications*, IEE Proc.-Electr. Power Appl, **151**, *1*, pp. 1–4 (2004).

8. N. Yongyuth, P. Viriya, K. Matsuse, *Analysis of a Full-Bridge Inverter for Induction Heating Using Asymmetrical Phase-Shift Control under ZVS and NON-ZVS Operation*, 7th International Conference on Power Electronics and Drive Systems., pp. 476–482 (2007).

9. I. Millan, D. Puyal, J. M. Burdio, C. Bemal, J. Acero, *Improved performance of half-bridge series resonant inverter for induction heating with discontinuous mode control*, IEEE Appl. Power Electron. Conf. Expo. – APEC., pp. 1293–1298 (2007).

10. A. Bhattacharya, P.K. Sadhu, A. Bhattacharya, N. Pal, *Voltage controlled hybrid resonant inverter – an essential tool for induction heated equipment*, Rev. Roum. Sci. Techn. – Électrotechn. Et Énerg., **61**, *3*, pp. 273–277 (2016).

11. A. Chakraborty, D. roy, T. K. Nag, P. K. Sadhu, N. Pal, *Open loop power control of a two-output induction heater*, Rev. Roum. Sci. Techn. – Électrotechn. Et Énerg., **62**, *1*, pp. 48–54 (2017).

12. C.M. Wang, H. J. Chiu, D. R. Chen, *Novel zero-current-switching (ZCS) PWM converters*, IEE Proc.-Electr. Power Appl, **152**, *2*, pp. 407–415 (2005).

13. A. Kumar, M. Sadhu, N. Das, P. K. Sadhu, D. Roy, A. Ganguly, *A Survey on High-Frequency Inverter and Their Power Control Techniques for Induction Heating Applications*, Journal of power technologies., **97**, *3*, pp. 201–203 (2017).

14. H.Y. Leung, D. Mccormick, D. M. Budgett, A. P. Hu, *Pulse density modulated control patterns for inductively powered implantable devices based on energy injection control*, IET Power Electronics., **6**, *6*, pp. 1051–1057 (2013).

15. H. N. Pham, H. Fujita, K. Ozaki, N, Uchida, *Dynamic analysis and control for resonant currents in a zone-control induction heating system*, IEEE Trans. Power Electron., **28**, *3*, pp. 1297–1307 (2013).

16. H. Sarnago, A. Mediano, O. Lucia, *High efficiency AC-AC power electronic converter applied to domestic induction heating*, IEEE Trans. Power Electron., **27**, *8*, pp. 3676–3684 (2012).

17. O. Lucia, J. Acero, C. Carretero, J.M. Burdio, *Induction heating appliances: Toward more flexible cooking surfaces*, IEEE Ind. Electron. Mag., **7**, *3*, pp. 35–47 (2013).

18. P. Kongsakorn, A. Jangwanitlert, *Fuzzy phase lock-loop for a two-output high frequency series-resonant induction heater*, TENCON IEEE Region 10 Conference., pp. 1–5 (2014).